Geosciences Journal
Vol. 13, No. 4, p. 423 − 432, December 2009
DOI 10.1007/s12303-009-0040-2

Three-dimensional surface wave tomography for the upper crustal velocity structure of southern Korea using seismic noise correlations

Jaehee Choi *School of Earth and Environmental Sciences, Seoul National University, Seoul 151-747, Republic of Korea*
Tae-Seob Kang *Department of Environmental Geosciences, Pukyong National University, Busan 608-737, Republic of Korea*
Chang-Eob Baag* *School of Earth and Environmental Sciences, Seoul National University, Seoul 151-747, Republic of Korea*

ABSTRACT: The cross-correlation technique was applied to ambient seismic noises to investigate the upper crustal velocity structure of the southern Korean Peninsula based on surface wave group velocities. We used seismograms recorded continuously during August 2005 at 91 accelerograph stations in the southern Korean Peninsula. From the correlation results of 4095 data pairs, the arrival times of Green's functions along paths between stations of pairs were measured in discrete bins of frequency bands with central frequencies of 0.15, 0.2, 0.25, 0.3, 0.35, 0.4, and 0.45 Hz. The spatial distribution of arrival times for each frequency band bin was inverted to obtain a two-dimensional tomographic map of Rayleigh wave group velocity. For each tomographic cell of the maps, we derived dispersion curves by extracting group velocities at center frequencies of the 7 frequency band bins. Shear-wave velocity obtained by depth inversion of the dispersion curve at each cell produced a one-dimensional velocity profile at depths. After aligning the profiles corresponding to tomographic cells, we obtained a three-dimensional uppermost crustal velocity model at depths down to approximately 8 km in the southern Korean Peninsula. These results show low-velocity distributions in the Gyeongsang Basin, western Gyeonggi Massif, and the area of Jeju Island and its northeastern coast. The Okcheon Fold Belt and Yeongnam Massif have relatively high velocity distributions. The low-velocity distribution in the Gyeongsang Basin shrinks in north-south direction at depths around 4 km and widens again with a tendency to migrate to the east as the depth is increased. However, the linear trend of low velocities in NNE-SSW direction at deeper depths (6.25–8.25 km) in the western area distinctively coincides with the western boundary of the Gyeongsang Basin. The background noise analysis in this study provided the constraining information for determination of depth variation in the shear-wave velocity distribution.

Key words: 3-D crustal velocity structure, seismic noise correlation, surface wave tomography, southern Korea

1. INTRODUCTION

Knowledge of the crustal structure is necessary for determining seismological source parameters, such as the focal depth and location of an earthquake. To obtain crustal information, seismologists have traditionally used ballistic waves emitted by earthquakes or explosions. However, the Korean Peninsula has moderate seismicity and thus experienced relatively few earthquakes that can provide key seismic information. Moderate to large earthquakes ($M_w > 4.0$) that can provide fundamental information, such as the travel times of body waves and dispersion curves of surface waves in and around the Korean Peninsula, occur less than ten times per year. Even in the case of small earthquakes which occur more frequently, it is hard to overcome the limitations inherent in the resulting information due to the uneven source distribution and uncertainties on the source parameters. On the other hand, about 100 digital seismic accelerometers have been available in southern Korea since the late 1990s (Fig. 1), and these instruments are continuously recording ground motions including so-called ambient seismic noise. This ambient seismic noise can provide us with information on the velocity structure along the path between stations of pairs. Therefore, utilizing these continuous records of the ambient seismic noise is an advantage over using earthquake data in southern Korea.

The cross-correlation technique is a valuable tool for extracting the Green's function from a random wavefield. An ultrasonic laboratory experiment showed a diffuse acoustic field to have a correlation equal to the Green's function of the medium (Lobkis and Weaver, 2001). Seismologists have attempted to extract Green's functions from interstation data through the cross-correlation of ambient ground motion with seismic coda, both experimentally (Campillo and Paul, 2003) and theoretically (Snieder, 2004). Subsequent studies have shown that this technique can be applied to ground noise as well as a scattered wavefield in an earthquake coda (Shapiro and Campillo, 2004; Weaver, 2005; Shapiro et al., 2005). For the southern Korean Peninsula, Kang and Shin (2006) conducted surface wave tomography using this technique with data from accelerograph networks in southern Korea for limited frequency bands (2–4 s), while Cho et al. (2007) used data from acceleration sensors as well as broadband sensors in the period range of 0.5–20 s.

In this study, we obtained shear wave velocity distribution maps at 17 depths down to approximately 8 km in the upper crust forming three-dimensional velocity structure by

*Corresponding author: baagce@snu.ac.kr

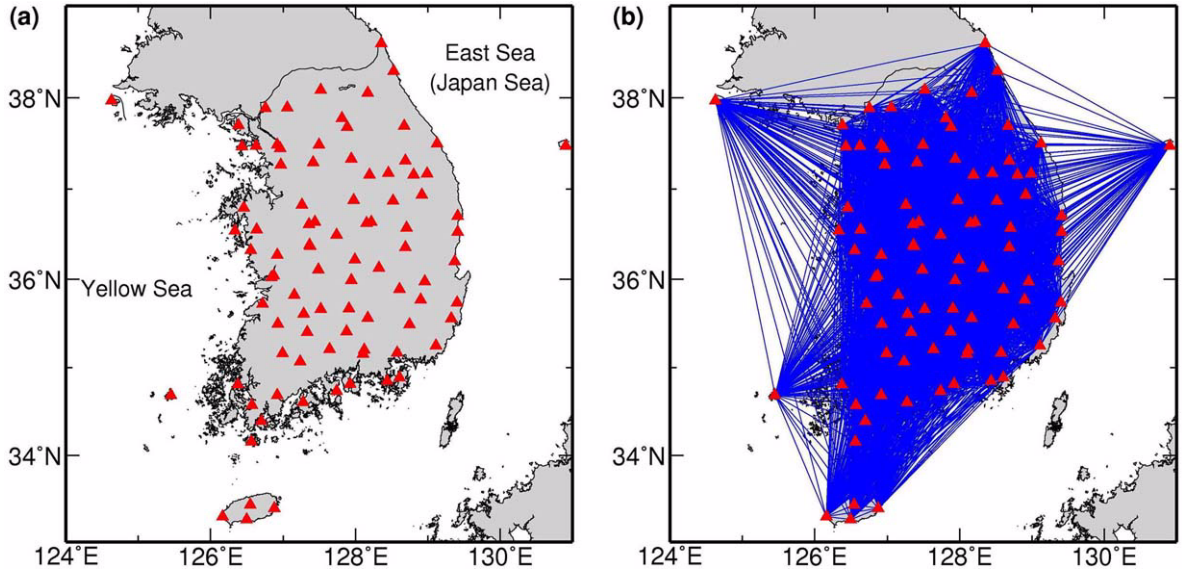

Fig. 1. Distributions of stations and ray paths. (a) Map showing locations of the 91 accelerograph stations of the seismic networks in the southern Korea. The networks are operated by Korea Meteorological Administration (KMA), Korea Institute of Geoscience and Mineral Resources (KIGAM), and universities. The curved line connecting the Yellow Sea and the East Sea in the northern area indicates Demilitarized zone between North Korea and South Korea. (b) Raypaths where surface wave group velocities are measured by correlating continuous seismic noise sequences recorded at individual pair of stations. The raypaths are assumed to be along the great circle path linking between stations of each pair and total 4095 (= 91 × 90/2) raypaths are shown.

analyzing extracted group velocity variations with frequency at two-dimensional tomographic cells. The group velocities were estimated from arrival times of surface wave Green's functions using the ambient seismic noise cross-correlation technique applied to continuously recorded accelerogram.

2. SEISMIC NOISE CROSS-CORRELATION

Crustal structures have been estimated using various methods based on seismic travel-time observations, crustal refraction profiles, and receiver function studies, etc. However, because of limited spatial sampling of data and uncertainties of the origin time and location of seismic source, these studies provided rough estimates of the three-dimensional crustal structure of southern Korea, especially for the shallow crust. The enhanced resolution of seismic images is mostly limited by the uneven distribution of seismic sources and receivers. Further, there are still some fundamental limitations in the resolution of seismic measurements from ballistic waves. Seismic surface waves are one of the main sources of information about the structure of the Earth's crust and upper mantle. However, measurements made from direct surface waves have several limitations. It is difficult to detect all directional signals, and inversions of ballistic surface waves require information about the source, which is not always known with sufficient accuracy. In addition, measurements made with teleseismic surface waves provide average values over the area of wave passages, which limits the resolution of resulting seismic images (Campillo and Paul, 2003). In contrast, diffuse wavefields are composed of waves propagating in all possible directions; therefore, these waves contain information about any possible path between receivers of pairs. The cross-correlation function of seismic ambient noise between a pair of distant stations is equivalent to the signal observed at one of the locations due to a surface point source acting at the other location (Snieder, 2004). Shapiro and Campillo (2004) also showed that the emerging Green's function signal from ambient seismic noise cross-correlation is dispersive, as expected for Rayleigh waves inside the Earth. This new type of surface wave measurement can provide information on velocity structures along numerous paths. Therefore, this method can significantly improve the resolution of seismic images for the purpose of this study.

Seismic noise consists mainly of surface waves, which are the elastic waves produced by the constructive interference of the P- and S-waves in the layers near the surface. Seismic noise can be classified into two large-scale parts of the frequency band. Low-frequency (0.01–0.5 Hz; 2–100 s) noises are generated by atmospheric effects, oceans, and solid earth, and can propagate hundreds of kilometers. High-frequency (about 1 Hz; 1 s) noises, such as those made by various human activities including traffic, construction work, and industry, are quickly attenuated. This type of noise can be observed at distances of several tens of kilometers (Aki and Richards, 2002). We are interested in microseisms, not cultural noises, which can be detected by accelerograph sensors over wide areas of southern Korea.

3. DATA PROCESSING

We used vertical component digital accelerograms recorded for one month in August 2005 in southern Korea. In total, 91 accelerograph stations have been operated by the Korea Meteorological Administration (KMA), Korea Institute of Geoscience and Mineral Resources (KIGAM), and various universities since the late 1990s. These stations are fairly uniformly and densely distributed in southern Korea, and thus the station pairs (Fig. 1) can provide a better-constrained high-frequency tomographic image of surface wave group velocities compared to traditional earthquake-based tomography suffering inevitably uneven source distribution, insufficient source information, and scattering at short-period part of waveforms.

The original data of accelerograms were recorded at a rate of 20 samples per second. However, as we wish to see only the effects of microseisms, which have spectral contents of frequencies lower than 1 Hz, we reformed the original data to the rate of 1 sample per second using a decimating technique. For efficiency of computation, the entire month of data was partitioned into 31 sections, each with a 1-day time period (Fig. 2a). To avoid the influence of large events in the correlation of noise sequences, we first removed the mean value and linear trend using the Seismic Analysis Code (SAC) program. Then, we removed the day trend by applying a high-pass filter, i.e., a two-pole two-pass Butterworth filter with a corner at 0.1 Hz (Fig. 2b). Finally, we divided the filtered data of the second step by the absolute values of the amplitudes in order to obtain a time series with only two amplitude values "–1" or "1" (Fig. 2c). Following this procedure, we created 91 noise data with 1-bit amplitudes and 1-day lengths by repeating the processing steps for all the stations.

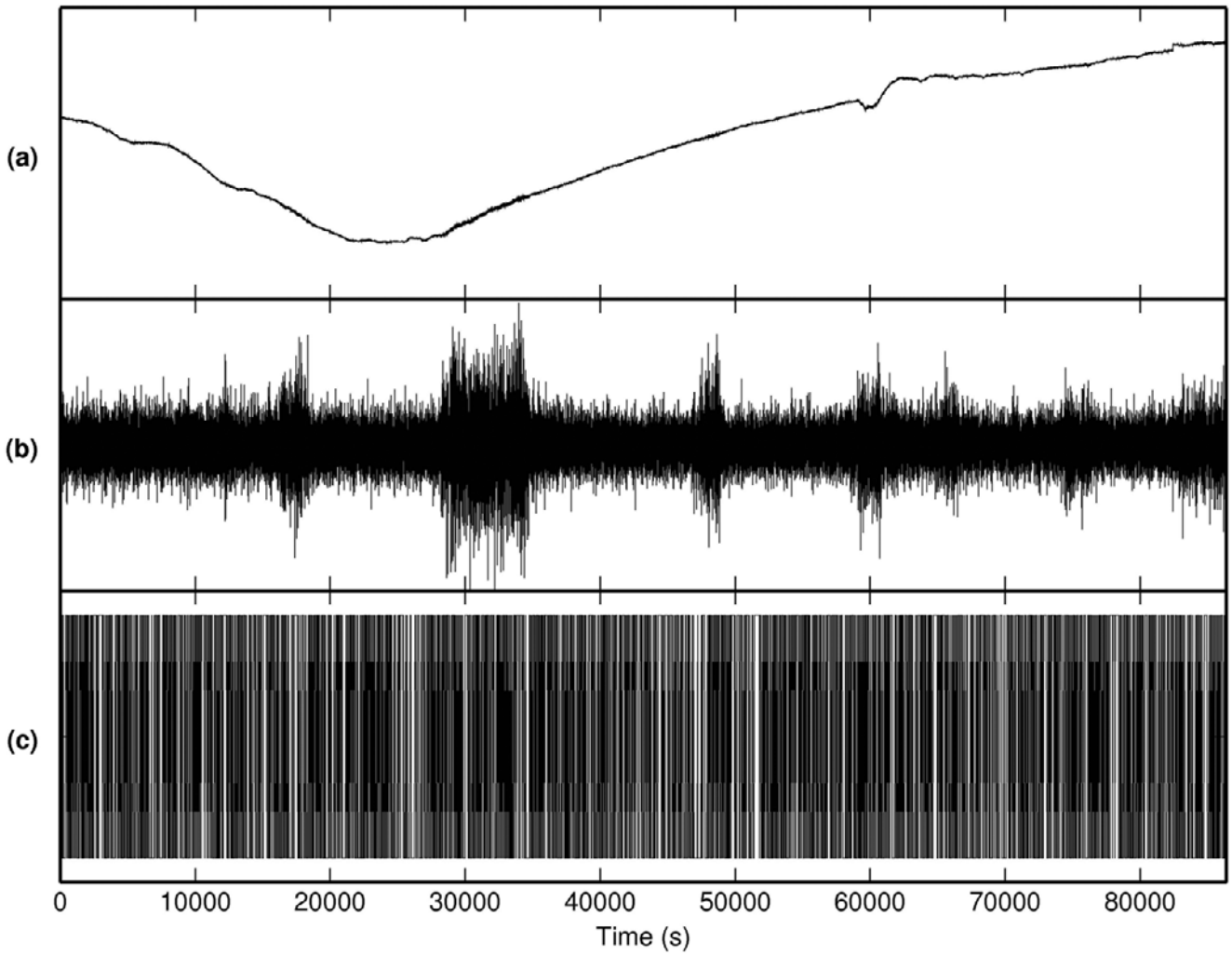

Fig. 2. Example of data processing: (a) raw seismogram of August 15, 2008 with 1 sample per second recorded during one day length at AND station, (b) result of high-pass filtering over 0.1 Hz after removing mean value and linear trend applied to the raw seismogram in (a), and (c) final one-bit seismogram which has only two amplitude values, "–1" or "1", obtained by dividing the filtered data by absolute value of amplitude in order to avoid influence of large events in the correlation of noise sequences.

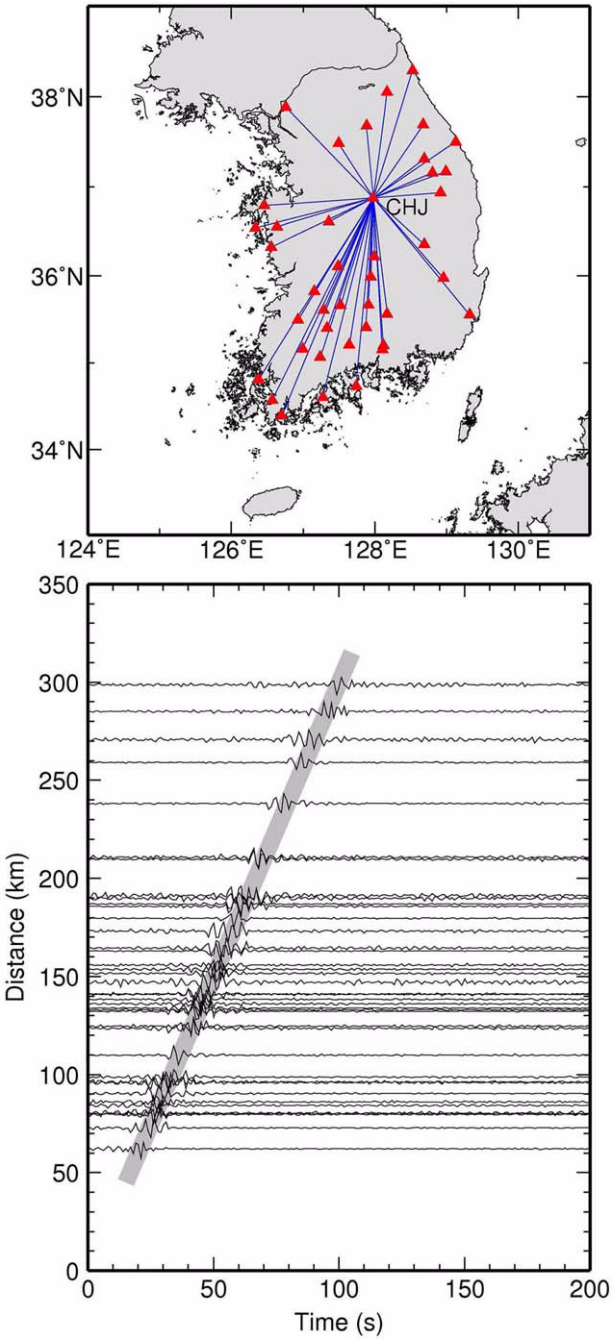

Fig. 3. A record section of symmetric-component cross-correlations using one month of data between station CHJ and other stations in the southern Korean Peninsula. The symmetric component is the average of the cross-correlation at time lags of causal (positive) and acausal (negative) parts. Traveltime-distance plot for a frequency band between 0.15 Hz and 0.25 Hz is shown on the bottom panel. The amplitude of each correlated-seismogram is normalized with respect to its maximum amplitude. Corresponding paths are denoted by solid lines on the top panel. The gray line on the bottom panel depicts the approximate arrival times for Rayleigh waves in this frequency band. For the traveltime tomographic inversion, the arrival time of Rayleigh waves in each correlated-seismogram is picked at the lag time of the signal corresponding to the maximum amplitude of envelope.

Each 1-bit noise seismogram corresponding to 1 day at a station was cross-correlated with those at other stations using the SAC (Seismic Analysis Code) program. For each pair of stations, we summed 31 cross-correlated seismograms of a month. Among the total 4095 stacked cross-correlation seismograms, we excluded traces with the signal-to-noise ratio (SNR: ratio of the maximum amplitude to the standard deviation of the entire trace) below 17 dB and those with station-to-station distance shorter than the three wavelengths. The number of resulting correlated seismograms is 1340 in total. To extract information in various frequency bands, we applied a Gaussian filter to the traces at the center frequencies of 0.15, 0.2, 0.25, 0.3, 0.35, 0.4, and 0.45 Hz. The surface wave group velocity was computed from the lag time of the maximum amplitude in each filtered correlated seismogram. In Figure 3, we show an example of the distance-time plot, where correlated seismograms are put at the station-to-station distance measured from station CHJ. Wave trains are clearly visible at a variety of azimuths with physically reasonable velocities of about 3.0 km/s. Since the vertical component seismograms were correlated for each pair of stations, resulting wave trains indicate Green's functions of Rayleigh waves which are polarized in the plane perpendicular to the free surface along the great circle path linking between individual pair of stations.

4. TWO-DIMENSIONAL TOMOGRAPHY OF RAYLEIGH WAVE GROUP VELOCITY

Rayleigh wave group velocity maps for bins of various frequencies were created by inverting group velocities of station pairs using the least-squares QR (LSQR) algorithm, which is a commonly used iterative method for solving large linear systems of equations and least-squares problems. We set a two-dimensional tomographic cell size of 12 × 12 km, considering the total area of southern Korea and number of correlation pair sets. From the damping test, we found that 100 was the best value for damping in LSQR algorithm tomography. Figure 4 shows results of the checkerboard test. The average number of paths through a cell (= number of cell hits) was 5. The reliable region for the tomographic map would be areas where the cell-hit count was above 10 (Fig. 5).

Computed spatially averaged group velocities over the whole area of southern Korea are 3.002, 3.005, 2.995, 2.984 2.987, 2.961, and 2.958 km/s at center frequencies of 0.15, 0.2, 0.25, 0.3, 0.35, 0.4, and 0.45 Hz, respectively (Fig. 6). There was a trend of slower Rayleigh wave group velocity with higher frequency. The computed tomographic maps of the seven frequency bands showed three remarkable low-velocity regions: the Gyeongsang Basin, the western part of the Gyeonggi Massif, and the southern Sea of Korea to the north of Jeju Island (Fig. 7).

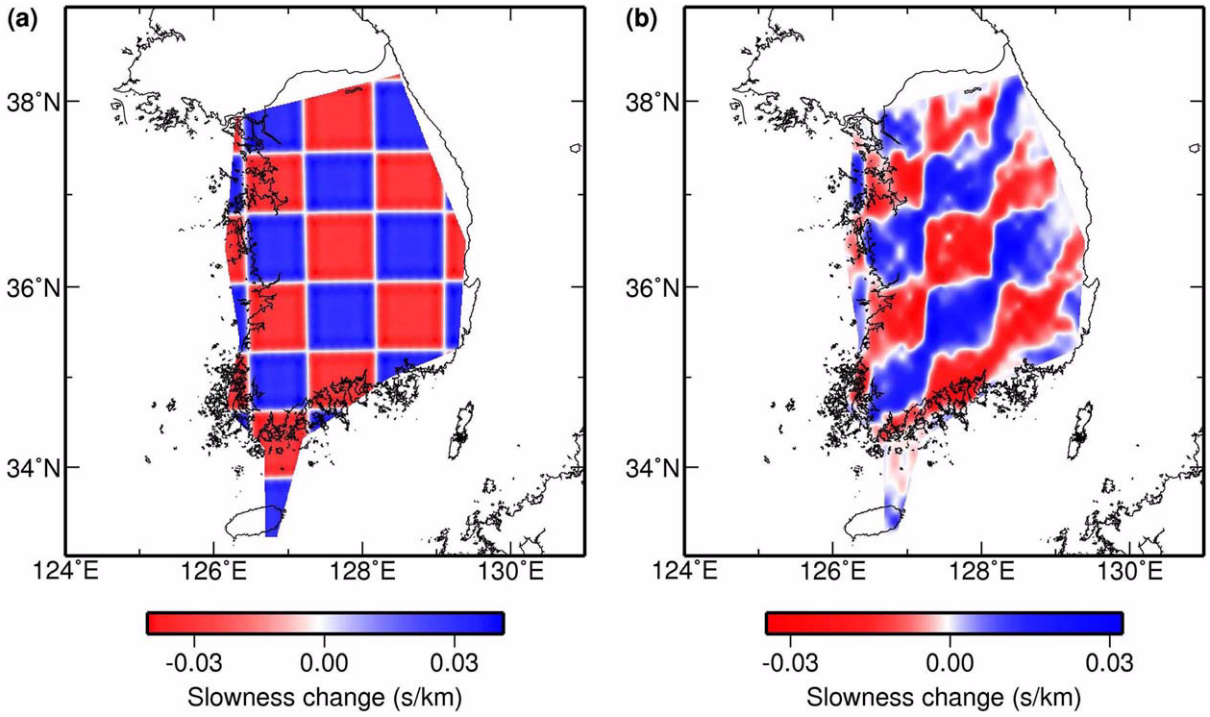

Fig. 4. Synthetic checkerboard resolution test. (a) Theoretical model which is composed of square cells of 80 km in length with ±0.03 s/km slowness alternation. (b) Inversion result for the scheme of square inversion cell with a size of 12 km in length and with damping value 100.

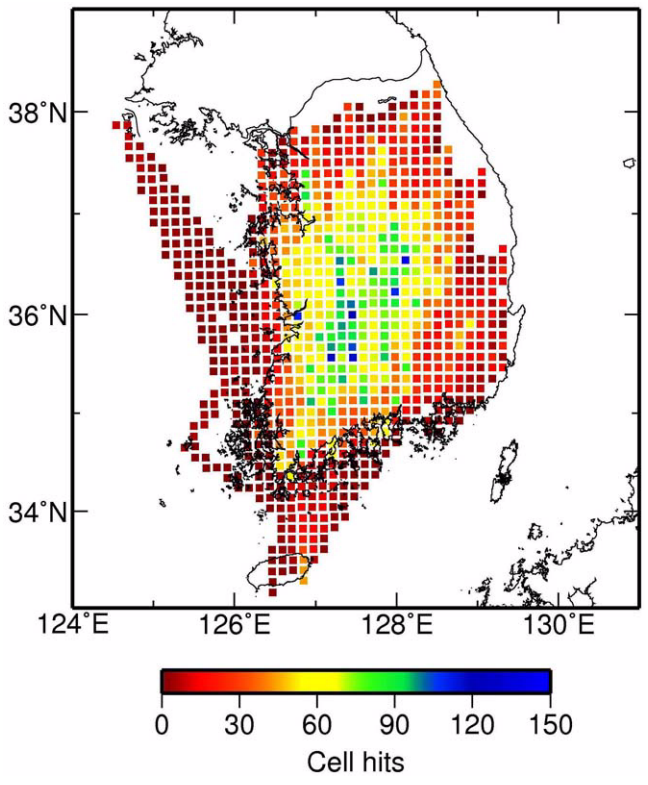

Fig. 5. Raypath density for a square cell size of 12 km in length. The raypath density is defined as the number of rays intersecting each square cell.

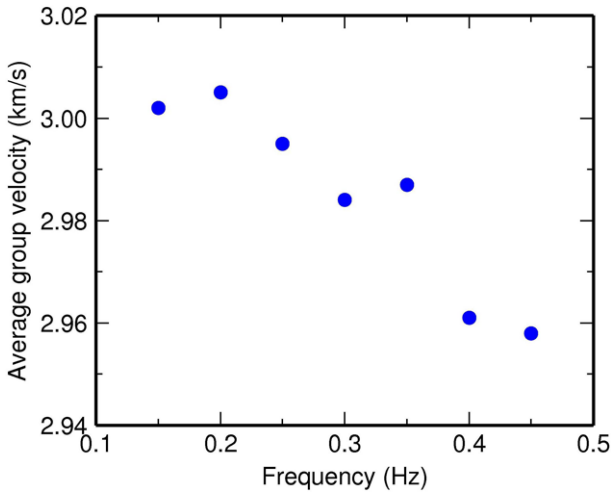

Fig. 6. Variation of the spatially averaged Rayleigh wave group velocities with respect to frequency over the whole area. There was a trend of decreasing Rayleigh wave group velocity with increasing frequency.

5. DEPTH INVERSION FOR THREE-DIMENSIONAL CRUSTAL VELOCITY MODEL

The maps of group velocity obtained in the previous section provide information on laterally varying Rayleigh wave velocities at different frequencies. For each grid cell, group velocities of the Rayleigh wave at seven frequencies (0.15 Hz,

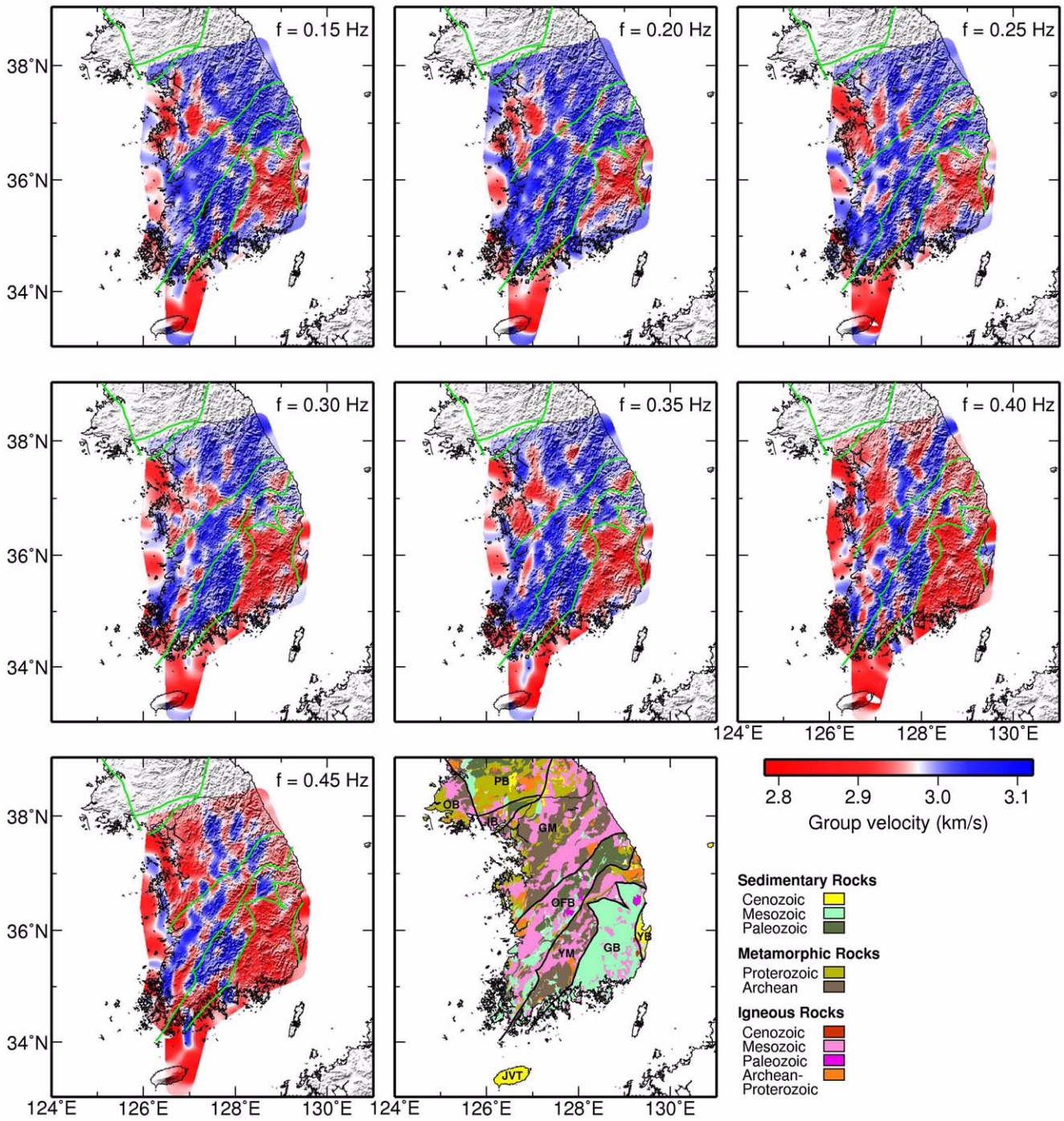

Fig. 7. Rayleigh-wave group-velocity tomographic maps at center frequencies of 0.15 Hz, 0.2 Hz, 0.25 Hz, 0.3 Hz, 0.35 Hz, 0.4 Hz, and 0.45 Hz, respectively. Frequency is indicated in the upper right corner of each map. The last panel shows a geological map with major tectonic provinces in the study area, which is modified from the geological and tectonic maps of Korea in a scale of 1:1,000,000 (Chwae et al., 1995; Hwang et al., 2001). The abbreviated names of geological provinces are (PB) Pyeongnam Basin, (OB) Ongjin Basin, (IB) Imjingang Basin, (GM) Gyeonggi Massif, (OFB) Okcheon Fold Belt, (YM) Yeongnam Massif, (GB) Gyeongsang Basin, (YB) Yeonil Basin, and (JVT) Jeju Volcanic Terrain.

0.2 Hz, 0.25 Hz, 0.3 Hz, 0.35 Hz, 0.4 Hz, 0.45 Hz) were extracted from the corresponding group velocity map, obtaining one dispersion curve for the cell. The dispersion curve constructed for each grid cell was then inverted to obtain one-dimensional shear wave velocity structures for depths using the surface wave inversion program Surf96 (Herrmann and Ammon, 2002). Surf96 conducts an iterative weighted inversion to find the structure velocity model.

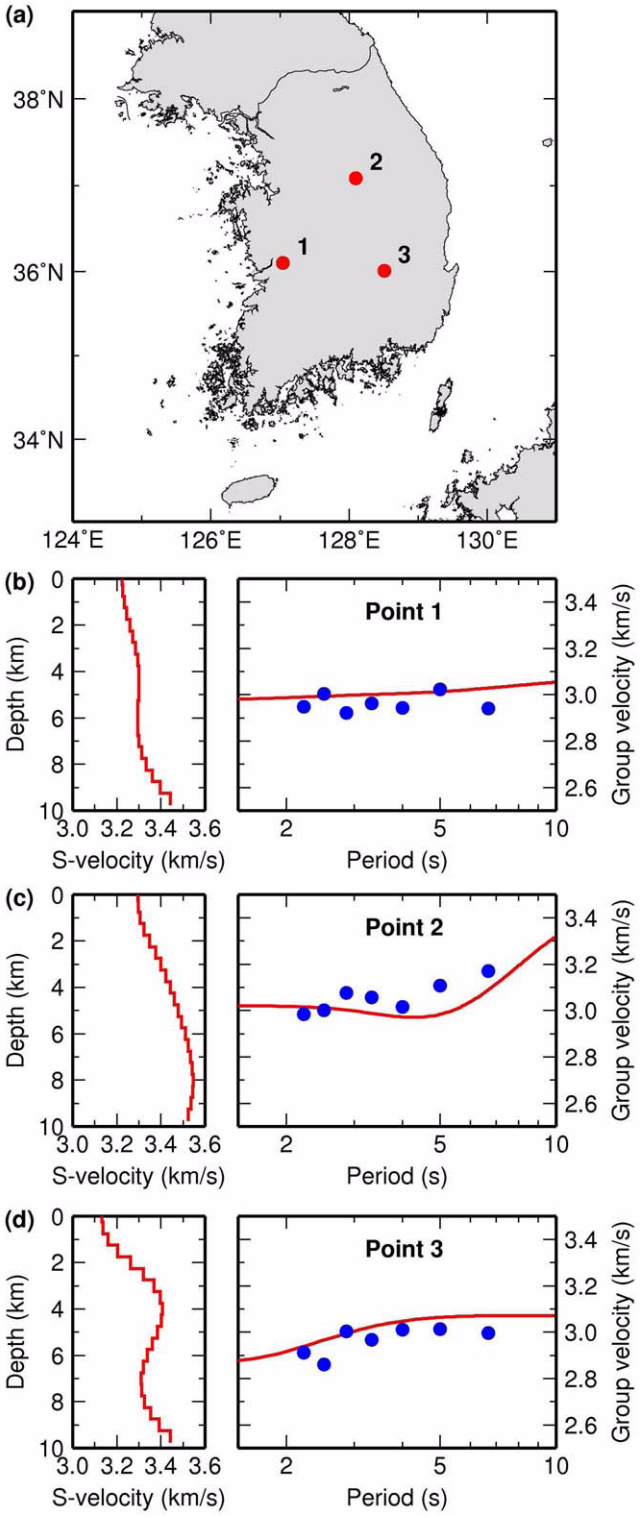

Fig. 8. Examples of the shear wave velocity profiles at three places obtained after inverting Rayleigh wave dispersion curves. (a) Map showing the location of the profiles. (b)–(d) Inversion of Rayleigh wave dispersion curve to the shear wave velocity profile at three points denoted in (a). The right panel shows the estimated Rayleigh wave dispersion relation (dots) and corresponding dispersion curves associated with the shear wave velocity profiles shown with solid line on the left panel.

The initial value of the shear wave velocity was set to 3.5 km/s, based on the report of Jung et al. (2007) who reported the shear wave velocity for the shallow crust of the southern Korean Peninsula obtained from short-period Rayleigh waves. The Poisson's ratio in each layer has been fixed during the inversion and the compressional-wave velocity was updated with constant density. From the resolution kernel, the reliable limit of depth inversion was shown to be approximately 8 km. The shear wave velocity distributions at 17 depths (0.25–8.25 km with a depth interval of 0.5 km) were computed using the Surf96 program with Rayleigh wave group velocity dispersion curves. Figure 8 shows three examples of the shear wave velocity profiles obtained at places of three surface grid cells of our tomographic model.

Figure 9 shows the final shear wave velocity structures at 17 depths from 0.25 km to 8.25 km with a depth interval of 0.5 km. Similar to the Rayleigh wave group velocity maps, remarkable low-velocity regions were detected for the Gyeongsang Basin, western part of the Gyeonggi Massif, and southern Sea of Korea to the north of Jeju Island at all depth levels. Especially, the low-velocity region in the Gyeongsang Basin seemed to shrink in north-south direction at depths around 4 km and widens again with a tendency to migrate to the east as the depth is increased. However, the linear trend of low velocities in NNE-SSW direction at deeper depths (6.25–8.25 km) in the western area distinctively coincides with the western boundary of the Gyeongsang Basin.

6. DISCUSSION AND CONCLUSION

This study obtained two-dimensional tomographic maps of Rayleigh wave group velocity with seven frequency bands (0.1–0.5 Hz) using cross-correlations of ambient seismic noise recorded by accelerograph networks in southern Korea. In addition, three-dimensional uppermost crustal S-wave velocity structure was obtained from depth inversion of dispersion curves constructed by extracting group velocities at center frequencies of seven frequency bands for each tomographic cell.

The general trends of Rayleigh wave group velocity maps for seven frequency bands in Figure 9 are similar to those of Kang and Shin (2006) and Cho et al. (2007). However, the three-dimensional uppermost structure computed in this study showed depth variation of the shear wave velocity distribution. The result could be obtained more precisely from densely and uniformly distributed accelerographs and careful inversion management in various frequency ranges. It is confirmed that, by obtaining the deterministic information on the surface-wave dispersions at high frequencies, the noise cross-correlation method with dense accelerograph data is a good way to deliver much better resolution regarding the upper crustal structure compared to traditional earthquake-based tomography.

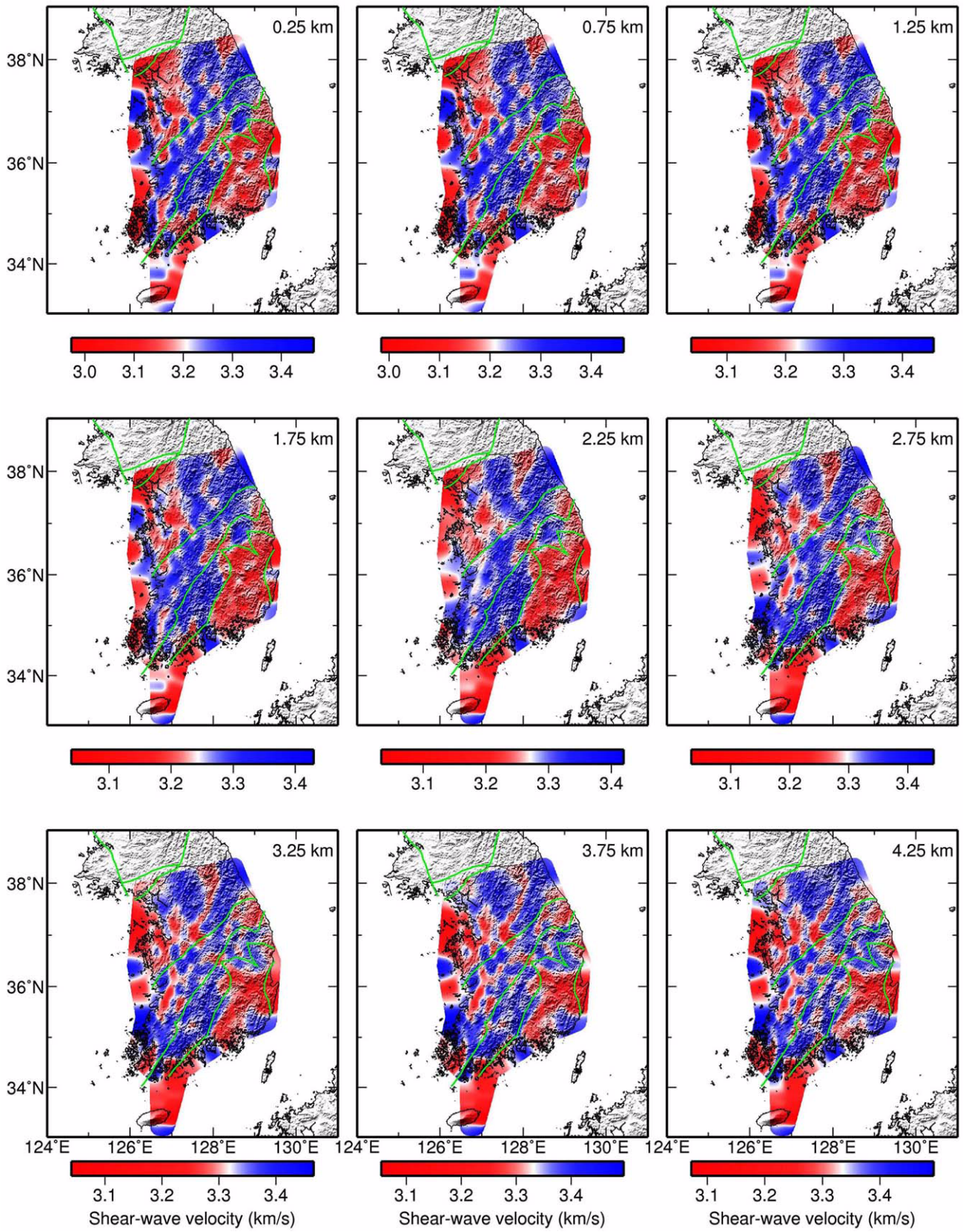

Fig. 9. Shear wave velocity distribution maps at 17 depths from 0.25 km to 8.25 km with 0.5 km interval. They were obtained by the inversion of dispersion curves at cell sites. The dispersion curves were constructed using Rayleigh-wave group-velocity tomographic maps at seven frequencies (Fig. 7). The depths in km are indicated in the upper right corner of each map.

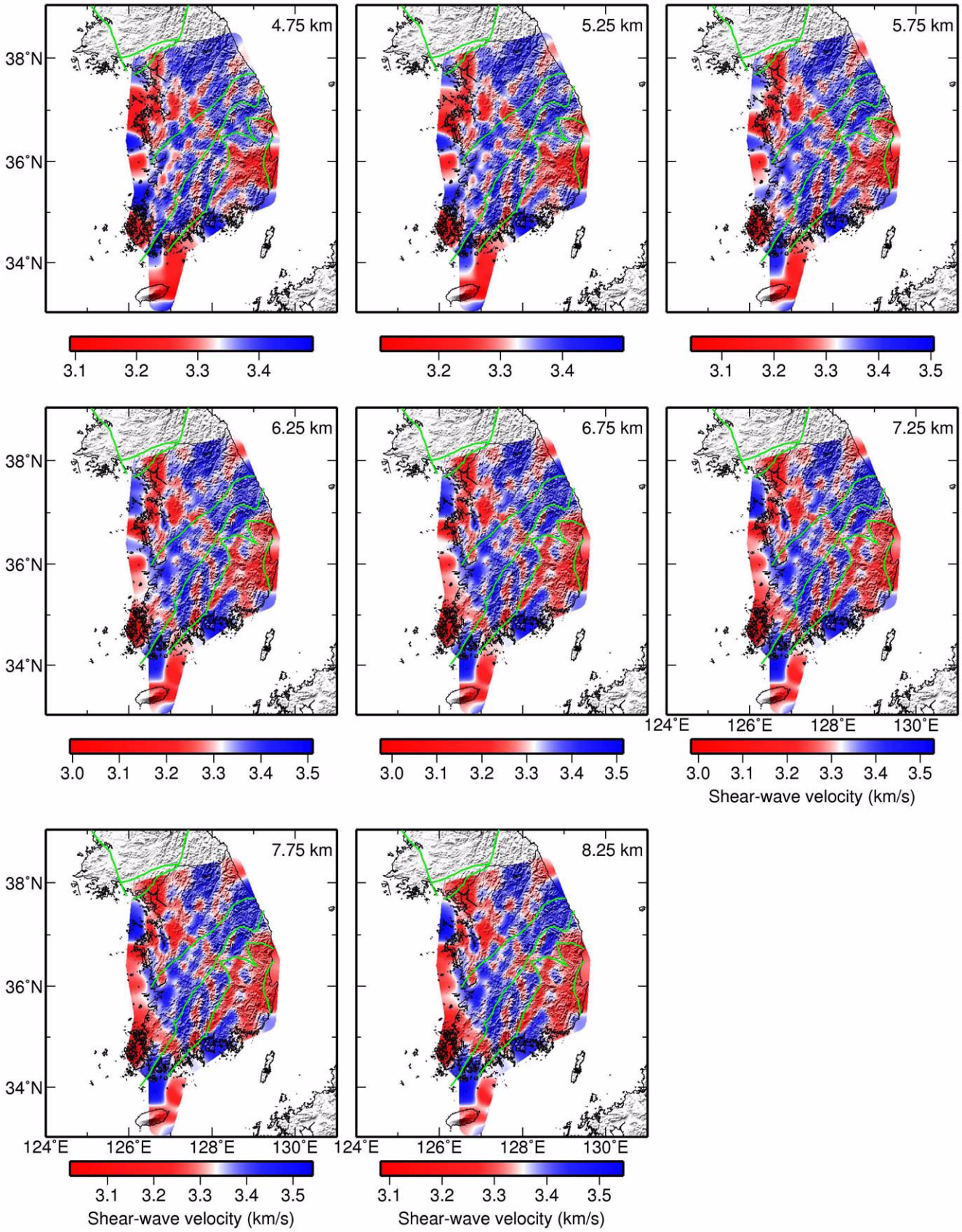

Fig. 9. (continued).

ACKNOWLEDGMENTS: This work was funded by the Korea Meteorological Administration Research and Development Program Grant CATER 2006-5205. We are grateful to the anonymous reviewers for their comments and suggestions.

REFERENCES

Aki, K. and Richards, P.G., 2002, Quantitative Seismology, 2nd edition. University Science Books, Sausalito, 704 p.

Campillo, M. and Paul, A., 2003, Long-range correlations in the diffuse seismic coda. Science, 299, 547–549, doi:10.1126/science.1078551.

Cho, K.H., Herrmann, R.B., Ammon, C.J., and Lee, K., 2007, Imaging the upper crust of the Korean Peninsula by surface-wave tomography. Bulletin of the Seismological Society of America, 97, 198–207, doi:10.1785/0120060096.

Chwae, U.C., Kim, K.B., Hong, S.H., Lee, B.J., Hwang, J.H., Park, K.H., Hwang, S.K., Choi, P.Y., Song, K.Y., and Jin, M.S., 1995, Geological Map of Korea, scale 1:1,000,000, Korea Institute of Geology, Mining and Materials, Daejeon, South Korea.

Herrmann, R.B. and Ammon, C.J., 2002, Computer Programs in Seismology, version 3.30, Saint Louis University.

Hwang, J.H., Jin, M.S., Jun, M.-S., Cho, J.D., Lee, S., Koo, S.B., Choi, P.-Y., Lee, Y.S., Kim, B.C., Kim, J.W., Kee, W.-S., Kang, P.C., Song, K.Y., Kim, J.H., Lee, S.R., and Chang, T.W., 2001, Tectonic Map of Korea, scale 1:1,000,000, Korea Institute of Geoscience and Mineral Resources, Daejeon, South Korea.

Jung, H., Jang, Y.-S., Lee, J.M., Moon, W.M., Baag, C.-E, Kim, K.Y., and Jo, B.G., 2007, Shear wave velocity and attenuation structure for the shallow crust of the southern Korean peninsula from short period Rayleigh waves. Tectonophysics, 429, 253–265, doi:10.1016/j.tecto.2006.10.003.

Kang, T.-S. and Shin, J.S., 2006, Surface-wave tomography from ambient seismic noise of accelerograph networks in southern Korea. Geophysical Research Letters, 33, L17303, doi:10.1029/2006GL027044.

Lobkis, O.I. and Weaver, R.L., 2001, On the emergence of the Green's function in the correlations of a diffuse field. Journal of Acoustic Society of America, 110, 3011–3017, doi:10.1121/1.1417528.

Shapiro, N.M. and Campillo, M., 2004, Emergence of broadband Rayleigh waves from correlations of the ambient seismic noise. Geophysical Research Letters, 31, L07614, doi:10.1029/2004GL019491.

Shapiro, N.M., Campillo, M., Stehly, L., and Ritzwoller, M.H., 2005, High-resolution surface-wave tomography from ambient seismic noise. Science, 307, 1615–1618, doi:10.1126/science.1108339.

Snieder, R., 2004, Extracting the Green's function from the correlation of coda waves: a derivation based on stationary phase. Physical Review E, 69, 046610, doi:10.1103/PhysRevE.69.046610.

Weaver, R.L., 2005, Information from seismic noise. Science, 307, 1568–1569, doi:10.1126/science.1109834.

Manuscript received August 7, 2008
Manuscript accepted December 10, 2009